Ocean Engineering 124 (2016) 135–140

Contents lists available at ScienceDirect

Ocean Engineering

journal homepage: www.elsevier.com/locate/oceaneng

Investigating sound speed profile assimilation: An experiment in the Philippine Sea

Cheng Chen, Bo Lei*, Yuan-Liang Ma, Rui Duan

School of Marine Science and Technology, Northwestern Polytechnical University, Xi'an, 710072 China

ARTICLE INFO

Article history:
Received 5 July 2015
Received in revised form
26 June 2016
Accepted 26 July 2016
Available online 4 August 2016

Keywords:
Sound speed profile
Assimilation radius
Multipath arrival delay
Correlation structure

ABSTRACT

In this paper, a single datum assimilation method is described for constructing the sound speed profile (SSP) in the ocean. Our method's key is assimilation radius, where various radii provide different SSPs. By means of the Bellhop acoustic model and acoustic data, we calculated the optimal SSP assimilation radius. Due to the lack of proper in-situ observations, an SSP inversion method is proposed. Inverted SSP compared to assimilated SSP indicates close correlation, showing that both methods yield reliable results. Historical data analysis indicates a stable correlation structure under certain conditions, implying the optimal assimilation radius would measure SSP effectively under similar conditions.

1. Introduction

SSP has great influence on underwater acoustic propagation, particularly sound transmission loss and multipath arrival structure. Thus, SSP greatly affects underwater activities like Anti-Submarine Warfare (Rui et al., 2012; Yan et al., 2007) and acoustic communication (Rouseff et al., 2001; Stojanovic et al., 1994). The ocean environment, particularly ocean temperature, which fluctuates continually, determines SSP. As well, when there exists ocean phenomena like internal wave or eddy, SSP can vary greatly even in a short time. Hence, it is necessary to address SSP estimation problems with data assimilation methods, called 'SSP assimilation'.

Much research has been conducted about the SSP assimilation issue with products like Modular Ocean Data Assimilation System (Fox et al., 2001) (MODAS) . Utilizing the three-dimensional variational (3D-VAR) method, the MODAS system predicts sea surface temperature via satellite data. The MODAS system has a database which contains the regression relationship between sea surface parameters and underwater parameters. Once 3-D temperature fields are calculated, corresponding salinity profiles according to a stable temperature-salinity relationship are obtained. Finally, the SSP of the area is within reach by means of an empirical formula for sound speed. Simple Ocean Data Assimilation (James et al., 2000) (SODA), on the other hand, is an ocean data assimilation product with averaged monthly 3-D temperature and salinity data. SODA starts with the Modular Ocean Model (Chen et al., 2003) (MOM), predicts dynamic ocean state, corrects the predicted field with measured data, and obtains the assimilated result. The Ocean Variational Analysis System (Jiang et al., 2007) (OVALS), developed by Zhu Jiang, brought about progress in the field of ocean data assimilation. Zhu's system uses the 3D-VAR method to perform data assimilation for each layer of the ocean. Assimilation parameters include both temperature and salinity. Researchers like Qingyu (2006) and Ying (2004) have studied the effect of mesoscale phenomena on acoustic propagation, including eddies, fronts, and internal waves. However, studies systematically applying ocean data assimilation on acoustic propagation are far from sufficient.

The key issue of SSP assimilation problem is the assimilation radius, with different radii providing different SSPs. Assimilation radius defines a range, within which the measured SSP can be used for SSP assimilation. If the assimilation radius is too small, there will be too few data available for SSP assimilation, resulting in assimilation result being easily corrupted by noisy SSP. If the assimilation radius is too large, too many data including those with low relevance to the target point will be used, leading to the assimilation result being smoothed.

An SSP assimilation experiment in the Philippine Sea was conducted, obtaining an optimal SSP assimilation radius. Data sources include SODA, Argo (Gould et al., 2004) (a daily data profile containing temperature and salinity), and acoustic data collected from an experiment conducted in the Philippine Sea in July of 2013. This paper proposes a method to obtain optimal SSP assimilation radius for SSP assimilation problems. First, we apply the Argo data to provide different SSPs with varied assimilation

* Corresponding author.
E-mail address: lei.bo@nwpu.edu.cn (B. Lei).

http://dx.doi.org/10.1016/j.oceaneng.2016.07.062
0029-8018/

radii. Since SSP affects the acoustic multipath arrival structure greatly, the measured acoustic multipath arrival data are used to find the SSP which best matches the acoustic data. The radius corresponding to this SSP is the optimal radius. Finally, by analyzing the correlation structure of that area, the optimal radius is tested for future SSP assimilation needs. An SSP inversion method was also performed. Results show that the inverted SSP and the assimilated one are in good agreement with each other, demonstrating both SSPs thus obtained are correct.

2. SSP profile assimilation

Sound speed C (m/s) is a function of temperature T (°C), salinity S (‰) and the static pressure P (kg/cm²) of the immediate ocean water column. By incorporating the pressure gradient dependencies of the Anderson equation into the Del Grosso equation and the Del Grosso–Mader dataset (Lovett, 1978), the equation is derived as follows.

$$C = 1449.22 + \Delta C_T + \Delta C_S + \Delta C_P + \Delta C_{STP}. \tag{1}$$

Here,

$$\Delta C_T = 4.6233T - 5.4585(10)^{-2}T^2 + 2.822(10)^{-4}T^3 - 5.07(10)^{-7}T^4$$

$$\Delta C_P = 1.60518(10)^{-1}P + 1.0279(10)^{-5}P^2 + 3.451(10)^{-9}P^3 - 3.503(10)^{-12}P^4$$

$$\Delta C_S = 1.391(S-35) - 7.8(10)^{-2}(S-35)^2$$

$$\begin{aligned}\Delta C_{STP} = {} & (S-35)\left[-1.197(10)^{-3}T + 2.61(10)^{-4}P - 1.96(10)^{-1}P^2 - 2.09(10)^{-6}PT\right] \\ & + P\left[-2.796(10)^{-4}T + 1.3302(10)^{-5}T^2 - 6.644(10)^{-8}T^3\right] \\ & + P^2\left[-2.391(10)^{-1}T + 9.286(10)^{-10}T^2\right] \\ & - 1.745(10)^{-10}P^3T\end{aligned}$$

From the above, it is shown that sound speed fluctuation depends mainly on temperature change. Sound speed fluctuation with temperature change is 4 m/s over 1 °C. Sound speed fluctuation with salinity is 1.14 m/s over 1‰. In the Philippine Sea area, based on the historical dataset, it is known that salinity fluctuates little, so we assume that it can be treated as a constant here due to its negligible effect. The SSP assimilation issue is thus reduced to an ocean temperature assimilation issue.

Since ocean environment is always in flux, and ocean data are sparsely sampled, it is difficult to obtain *in-situ*-measured data for all specified points we call targets. Temperature assimilation method is an effective way to estimate temperature profiles. The reason lies in this method's mechanism which employs all points near the target both in time and space, based on their correlation. Closer points are given greater weight according to their higher correlation.

Argo data close to the target profile both in time and in space within a specific range served as our source for assimilation. We then calculate the assimilated temperature profile.

$$T_{DA} = \sum_{i=1}^{P} T_i \times \alpha_i \times W_i, \tag{2}$$

$$W_i = \exp[-(l_x/L_x)^2 - (l_y/L_y)^2 - (l_t/L_t)^2], \tag{3}$$

$$\alpha_i = W_i / \sum_{i=1}^{P} W_i, \tag{4}$$

where T_{DA} is the assimilated temperature profile. T_i is the temperature profile of Argo data. Within the specific range, there are a total of P available temperature profiles. Weighted coefficients are symbolized as α_i. W_i stands for correlation coefficients between Argo points and the target. The longitudinal distance between Argo points and the target is represented by l_x. l_y is the latitudinal distance. l_t is the time lag between Argo points and the target. L_x is the longitudinal correlation distance. L_y is the latitudinal correlation distance. L_t is the timescale to define correlation in time domain.

Both for convenience and in response to the character of ocean phenomena (Fox et al., 2001), one month is the selected timescale here. Represented by assimilation radius, the spatial range requires careful study. Since the ocean variation in the latitudinal direction is much larger than that in the longitudinal direction and to simplify the study of assimilation radius, we assume that the longitudinal correlation distance is two times of the latitudinal correlation distance for convenience. Thus, the issue of assimilation radius is reduced to the issue of latitudinal radius. We describe later our search for optimal radius through Argo data and *in-situ*-measured acoustic data.

3. Philippine Sea experiment and discussion

3.1. Philippine Sea assimilation experiment

Collected in Philippine Sea in July of 2013, our data come from Argo and the measured acoustic data. Here, the Argo data are selected from June and July of 2013, at a site near the location where the acoustic experiment was conducted. The vertical water column data range is from surface to a depth of 2000 m. Since temperature variation is very weak in deep water layers, we assume a constant SSP gradient below 2000 m depth here. Temperature profiles near the target location are almost constant below 1100 m, but vary largely above that depth, as shown in Fig. 1. Hence, by averaging all the temperature profiles of this area, we obtain an estimated profile for depths from 1100 m to 2000 m. But when the averaged profile is connected with the assimilated profile at shallower depths, a discontinuity may occur. Two weighting coefficients $k_A(z)$ and $k_W(z)$ are introduced to merge the two profiles smoothly. The profile merging formula is (5)–(7).

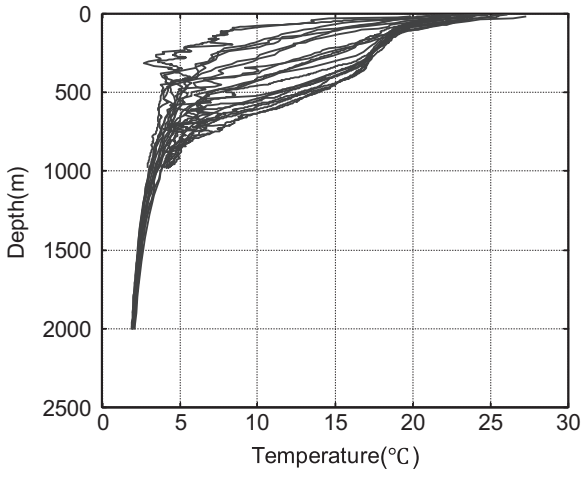

Fig. 1. Argo temperature profiles. The temperature profiles are of the same day, and their locations spread near the target point.

$$t = \begin{cases} t_A(z), & z < Z_u \\ k_A(z) \bullet t_A(z) + k_W(z) \bullet t_W(z) & Z_u \le z \le Z_d \\ t_W(z) & z > Z_d \end{cases} \quad (5)$$

$$k_A(z) = \frac{Z_d - z}{Z_d - Z_u} \quad (6)$$

$$k_W(z) = \frac{z - Z_u}{Z_d - Z_u} \quad (7)$$

Here, t_A refers to the assimilated profile, t_W refers to the averaged profile and t refers to the merged profile. Z_u is chose 800 m. Z_d is chose 1100 m. According to the formula, new profiles above Z_u are provided by assimilated profile, while profiles below Z_d are provided by averaged profile. The overlapping part is provided by both profiles, and if it is closer to the surface, the weight of assimilated profile is larger; if it is closer to the bottom, the weight of averaged profile is larger.

We collected acoustic data at the coordinate (20°, 137°) , and a depth of 4700 m. The deepest point of the target area is 4936 m and in-situ measured data suggest a flat bottom at the experiment area. The acoustic source signal comes from a depth of 200 m. A sketch map of the acoustic experiment is shown in Fig. 2. Based on historical dataset, salinity is assumed to be a constant 35‰.

The measured multipath arrival delay is as shown in Fig. 3. According to the Snell theorem, SSP fluctuation can little affect the near-range propagation including the multipath arrival structure, but has great effect on long-range propagation (Rui et al., 2013). Experiments show that as long as the basic structure of SSP is determined, SSP fluctuation will not have obvious effect on the multipath arrival delay structure within a certain range, but the structure outside that range will be sensitive to fluctuations. Given that we focus on the effect of SSP fluctuation on multipath arrival structure, we need to figure out the range. Acoustic simulations that were carried out suggest that the range of 20 km is a proper choice for our case in the deep ocean. Thus, the multipath arrival delay beyond the range of 20 km served as the study object.

With Argo data and the acoustic data, we conducted an experiment, resulting in the flow diagram shown in Fig. 4. From various assimilation radii, we obtain different SSPs. By means of the Bellhop model, the SSP determines a multipath arrival structure, which is compared with the measured data. That estimate showing the minimal difference between the two structures we consider optimal, and the corresponding radius is the optimal assimilation radius. The difference between the two structures is constructed here.

$$J = \sum_{l=1}^{N} \left[(R_l - r_l)^2 + (D_l - d_l)^2 \right] \quad (8)$$

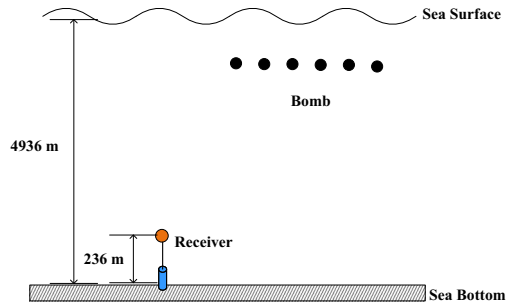

Fig. 2. Sketch map of the acoustic experiment.

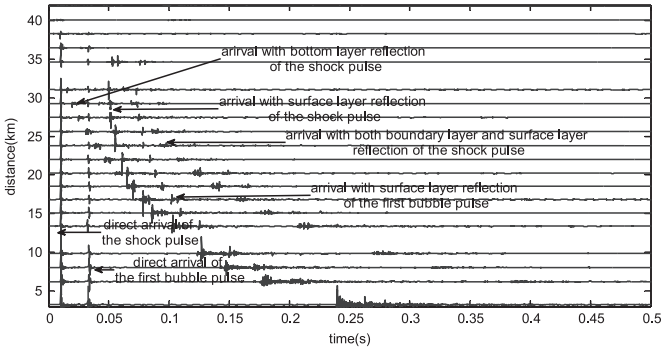

Fig. 3. Measured multipath arrival delay. The multipath arrival delay is the relative delay, which means that all delay is presented less the direct arrival time, and plus a small number for better viewing. The figure includes both the shock pulse and first bubble pulse signal arrivals. The amplitude of first explosion arrivals is much larger than the second. Arrival structure includes one-time surface reflection, one-time bottom reflection, and one-time surface layer and bottom layer reflection.

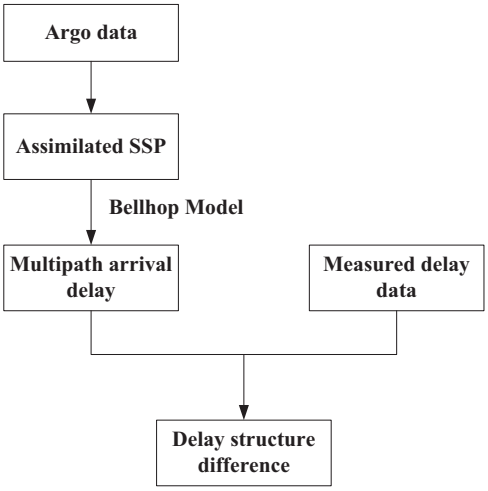

Fig. 4. Flow diagram of SSP assimilation acoustic experiment. Argo data are assimilated to give the SSP. Then SSP is used as the input on a Bellhop Model, which yields the multipath arrival delay as its output. The calculated delay is then compared with measured delay data.

J represents the objective function value of the difference. N is the number of measured values. R_l is the simulated value of the distance from source to receiver; r_l is the measured value. D_l is the simulated value of multipath arrival delay, and d_l is the measured one. Arrival delay is still the relative delay compared to the direct arrival delay. Since the objective function value J is constructed to compare the structures of multipath arrival delay as shown in Fig. 2, and J is constructed with two types of variables with different units (R, 'km' D, 's'), to avoid the case that one variance are much larger than the other one, a scaling factor of 100 is used to enlarge the value of multipath arrival delay.

3.2. SSP inversion

To invert SSP, the empirical orthogonal function (EOF) method (Bilan and Xuejia, 1981) is employed first to decompose Argo data giving us the eigenvectors which correspond to large eigenvalues. By simulated annealing method, we calculate the best coefficients for EOF, and the SSP for that area is obtained.

In the Philippine Sea, we selected a square area from which we used Argo data for analysis. The ocean temperature field is represented as M, which is a $p \times q$ matrix, where p is the number of layers of the ocean temperature field and q is the number of points. We then employ EOF to decompose M thus:

$$R = M \times M', \tag{9}$$

$$(R - \lambda I)K = 0. \tag{10}$$

R is the covariance matrix of M. The eigenvalue for R is λ. K is the empirical orthogonal matrix, which is a $p \times p$ matrix. Since the first three large eigenvalues account for 98.3% of the total eigenvalues, indicating the corresponding EOF vectors can explain 98.3% of the variability in the data, the first three EOF vectors are chose to represent temperature profile of any point in this area.

$$T = \alpha_0 + \alpha_1 k_1 + \alpha_2 k_2 + \alpha_3 k_3. \tag{11}$$

Here α_0 is a constant coefficient, and α_1, α_2, α_3 are the respective coefficients corresponding to each empirical orthogonal function. k_i corresponds to each empirical orthogonal function. With the measured multipath arrival delay data, the best coefficients can be obtained by means of simulated annealing method (Zhongbing et al., 2005). The objective function is constructed the same as the one in Eq. (8) in Section 3.1.

Once the temperature profile is obtained with the coefficients calculated, the inverted SSP can be acquired by means of the SSP empirical formula.

3.3. SSP assimilation

As described in part I, different SSPs result from different assimilation radii. The multipath arrival delay can be calculated through the Bellhop model with this SSP. Then the result is compared with the measured delay. The total variance between the calculated delay structure and the measured one is used to describe the effects of the assimilation radius on multipath arrival delay estimation, as shown in Fig. 5a. The corresponding number of Argo profiles used is shown in Fig. 5b.

Fig. 5a shows results for a small radius, there will be some singular values which appear to be large. This is because too few data are available to conduct temperature assimilation, resulting in noise from one region affecting the assimilation result greatly. When the longitude radius reaches 500 km, latitude radius 250 km, the total variance approaches minimum. Thus the preceding radius could be considered an optimal radius for temperature assimilation in that area, and the temperature profiles are strongly correlated within this range. Yet, the radius should not be excessively large. If a chosen radius is too great, an excessive number of Argo data for assimilation will result. The assimilation process would then include large numbers of irrelevant data whose correlation with the target point is poor. As a result, the true temperature profile would be smoothed. Even though the total variance would approach a steady value, the assimilated temperature profile would deviate from the real one.

One assimilated SSP, whose corresponding total variance is 2.5, is shown in Fig. 6a. Compared with the inverted SSP, the two essentially agree with each other with a difference 102 measured by the following equation:

$$Dssp = \sum_{k=1}^{L} |Assp(k) - Issp(k)| \tag{12}$$

Difference between the assimilated SSP and the inverted SSP is measured by $Dssp$, $Assp(k)$ represents the assimilated sound speed of the k th layer, while $Issp(k)$ represents the inverted sound speed of the kth layer. There are a total of L layers. In this experiment, the upper 120 layers ranging from the surface layer to a depth of 1200 m is chose for study.

A multipath arrival delay calculated from the assimilated SSP in Fig. 6a agrees with the measured one, as shown in Fig. 7a. If the total variance is larger than 5, the calculated multipath arrival will deviate from the measured one seriously, as shown in Fig. 7b, in which the total variance is 6. Compared to the inverted SSP, the assimilated SSP deviates largely at depths above 1100 m with a difference 524, shown in Fig. 6b.

4. Correlation structure analysis of temperature field

Our assimilation method is based on the correlation between different points in temporal and spatial domains. Optimal assimilation radius defines a range within which we assume there is significant relevance. Correlation structure of temperature field determines the optimal assimilation radius for a specific region. Thus, the stability of the correlation structure of temperature field determines the possibility of assimilation radius for future SSP assimilation.

We used SODA data for the same month 1996–2005 to construct temperature field correlation structure analyses. The SODA temperature field is a three-dimensional field with 26 depth layers in total. We chose an area with the longitudinal range (124°, 144°), and the latitudinal range (12°, 32°).

First, we constructed the temperature field correlations for each of 26 layers in the same month over ten years. When

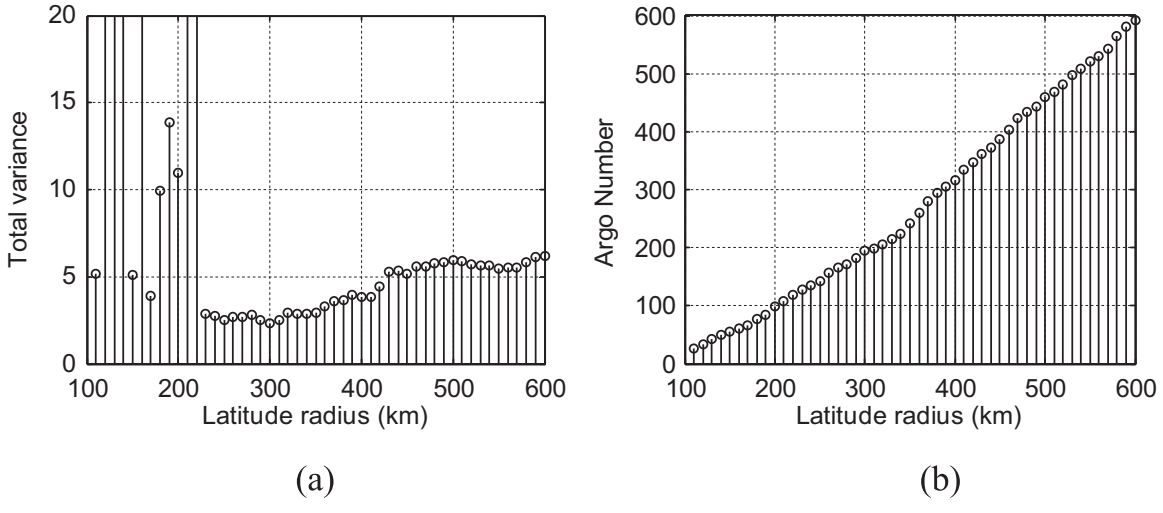

Fig. 5. (a) Difference between the measured multipath arrival delay and the simulation results from the assimilated SSP calculated from different assimilation radii. The Argo data used are within the assimilation radius. (b) The corresponding number of Argo profiles.

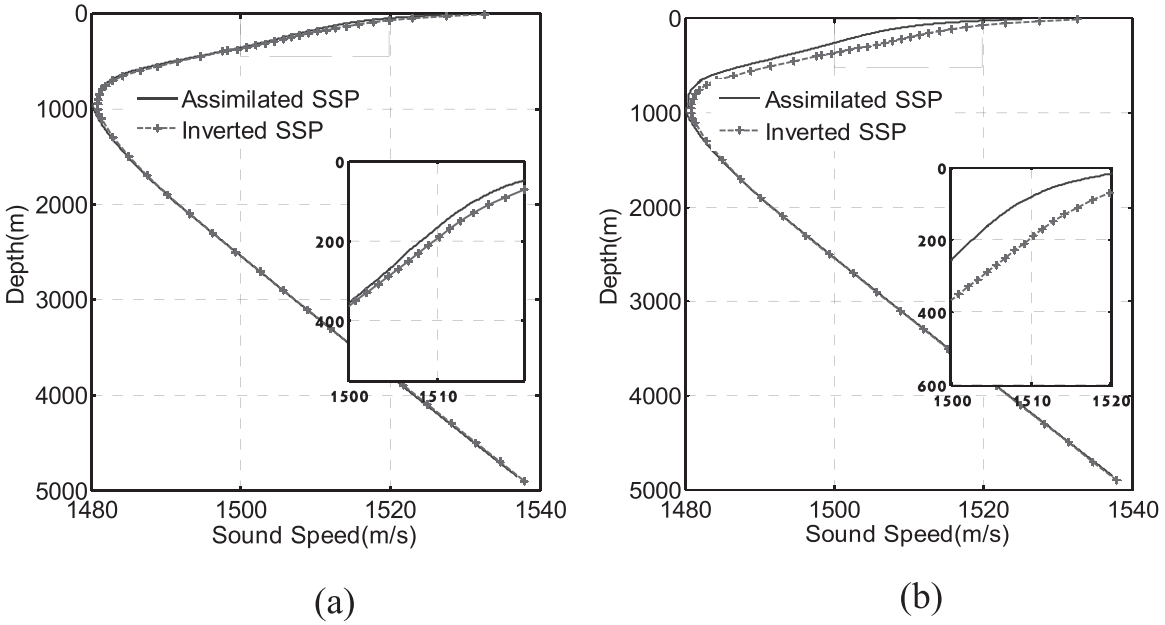

Fig. 6. (a) assimilated SSP with a longitude radius of 500 km and latitude radius 250 km and the inverted SSP, (b) assimilated SSP with longitude radius 1000 km and latitude radius 500 km and the inverted SSP.

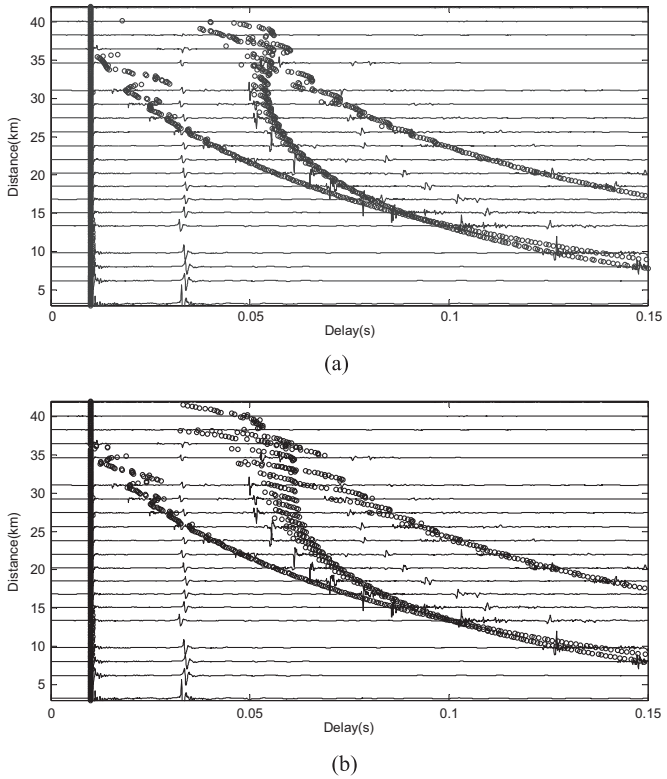

Fig. 7. (a) The multipath is derived using the assimilated SSP in Fig. 6 (a) Comparison of the simulated multipath arrival delay structure with measured ones. Here, the assimilation radius is longitudinal 500 km and latitudinal 250 km. (b) Comparison of the simulated multipath arrival delay structure with measured ones. Here the assimilation radius is longitudinal 1000 km and latitudinal 500 km. Within the distance of 20 km, the multipath arrival delay structure remains stable, yet the structure is sensitive to SSP fluctuations over distances larger than 20 km, as shown in the two figures here.

comparing the temperature field correlation structure of the same layer and the same month, the correlation structure remains basically stable. Fig. 8 illustrates top-layer field correlation structures for June, randomly selected from the 10 years. The figures clearly show that correlation structure remains essentially unchanged across the 10 years. What's more, the figures illustrate the assumption that there is significant relevance within the optimal assimilation radius obtained from previous context. There is strong relevance within the rectangle defined by the assimilation radius, and the relevance decays steeply out of the range.

Next, to obtain a more accurate answer as to correlation structure stability, we performed another analysis on the similarities of these structures. Again, we selected the group of correlation structures from the same layer and the same month. Since correlation values near the diagonal axis reflect the major structure characteristics, we selected region near the diagonal axis to study correlation structure similarities.

We then calculated the correlation coefficients of adjacent years. The larger the correlation coefficients, the more similar the two structures are. After analyzing all the groups for the 26 layers and 12 months, results indicate that they are similar to each other in most cases despite some singular values. For these singular values, possible explanations are the fact that ocean climate is in constant flux and extreme weather occurs. Table 1 lists the correlation coefficients of adjacent years for the top-layer structure group in June across the 10 years.

Thus, the temperature field correlation structure remains relative stable. As a result, the optimal assimilation radius remains stable under similar conditions and can be used for SSP assimilation calculations on the same month for this area in the future.

5. Conclusion

We conducted an ocean data assimilation experiment in the Philippine Sea to find an optimal assimilation radius for a given selected ocean area. When the corresponding SSP calculated from such a radius is compared with its inverted SSP, results show they are consistent with one another. Our results support both methods as effective and valid, since different mechanisms of method give the same result. Finally, we demonstrate the usefulness of the optimal assimilation radius for future assimilation issue by means of a correlation structure analysis.

It is important to note that the inverted SSP or the assimilated

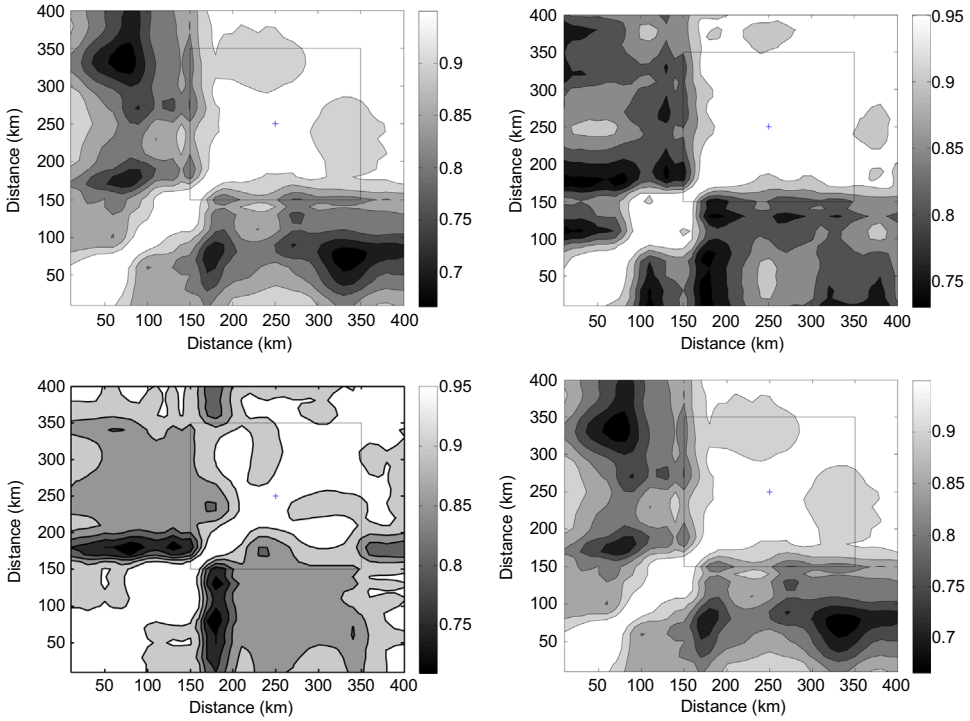

Fig. 8. Correlation structures constructed from SODA data of the same month. The above four are chose randomly from the ten year span. The '+' symbol indicates the location where the acoustic experiment was conducted. The rectangle here is defined by the assimilation radius obtained in the previous context.

Table 1
Correlation coefficients of adjacent years.

	1–2	2–3	3–4	4–5	5–6	6–7	7–8	8–9	9–10
Correlation	0.905	0.727	0.720	0.765	0.678	0.633	0.741	0.832	0.888

SSP should not be viewed as the exact SSP solution for that particular area, since the ocean environment is always a range-dependent one, where SSPs have fluctuations. As an average for the whole area such SSPs remain valuable, because physical phenomena of the ocean possess large-scale characteristics. Further research, like ocean meso-scale phenomenon parameterization (Zhuhui et al., 2014), is needed to investigate range-dependency and SSP solutions over the entire study area.

Acknowledgement

This work is supported by the National Natural Science Foundation of China (61101192), the Foundation of State Key Lab of Acoustics, Chinese Academy of Sciences (SKLA201301), the Science and Technology on Underwater Test and Control Laboratory (9140c260201130c26096), NPU Foundation for Fundamental Research (NWPU-FFR-JCY20130111), and Yang Talent Project (2015JQ5199).

References

Rui, Duan, Kun-De, Yang, Yuan-Liang, Ma, Bo, Lei, 2012. Research on reliable acoustic path: physical properties and a source localization method. Chin. Phys. B 21 (12), 124301.

Wang, Yan, Wan, Qun, Bai, Danping, Jiang, Jin, 2007. Acoustic localization in multi-path aware environments. In: Proceedings of the International Conference on communications, circuits and systems, ICCCAS 2007, 11, 13, pp. 667–670.

Rouseff, D., Jackson, D.R., Fox, W.L.J., Jones, C.D., Ritcey, J.A., Dowling, D.R., 2001. Underwater acoustic communication by passive-phase conjugation: theory and experimental results. IEEE J. Ocean. Eng. 26 (4), 821–831.

Stojanovic, M., Catipovic, J.A., Proakis, J.G., 1994. Phase-coherent digital communications for underwater acoustic channels. IEEE J. Ocean. Eng. 19 (1), 100–111.

Fox, D.N., Tegue, W.J., Barron, C.N., Carnes, M.R., Lee, C.M., 2001. Modular ocean data assimilation system. J. Atmos. Ocean. Technol. 19, 240–252.

Carton, James A., Chepurin, Gennady, Cao, Xianhe, 2000. A simple ocean data assimilation analysis of the global upper ocean 1950-95. Part I: methodology. J. Phys. Oceanogr. 30, 294–309.

Chen, C., Liu, H., Beardsley, R.C., 2003. An unstructured grid, finite-volume, three-dimensional, primitive equations ocean model: application to coastal ocean and estuaries. J. Atmos. Ocean. Technol. 20 (1), 159–186.

Jiang, Zhu, Guangqing, Zhou, Changchun, Yan, Weiwei, Fu, Xiaobao, You, 2007. The design and primary application of a three dimensional ocean data assimilation system. Sci. China 37 (2), 261–271.

Qingyu, Liu, 2006. The Acoustic Propagation in Ocean Mesoscale Phenomenon. Harbin Engineering University, Harbin.

Ying, Kang, 2004. The Analysis of the Acoustic Propagation Characteristic in Ocean Mesoscale Structure. Ocean University of China, Qingdao.

Gould, J., Roemmich, D., Wijffels, S., et al., 2004. Argo profiling floats bring new era of in situ ocean observations. Eos Trans. Am. Geophys. Union 85 (19), 185–191.

Lovett, J.R., 1978. Merged seawater sound-speed equations. J. Acoust. Soc. Am. 63 (63), 1713–1718.

Rui, Duan, Kun-De, Yang, Yuan-Liang, Ma, 2013. Investigation of long-range sound propagation in surface ducts. Chin. Phys. B 22 (12), 124301.

Bilan, Du, Xuejia, Song, 1981. The method of applying EOF to analyse and predict the sea surface temperature. Acta Oceanol. Sin. 3 (1), 14–27.

Zhongbing, Zhang, Yuanliang, Ma, Kunde, Yang, 2005. The matched beam inversion method of sound speed profile in the shallow sea area. Acta Acust. 30 (2), 103–107.

Zhuhui, Jiang, Sixun, Huang, Xiaobao, You, Yiguo, Xiao, 2014. Ocean internal waves interpreted as oscillation travelling waves in consideration of ocean dissipation. Chin. Phys. B, 05.